Molecular Biology of the Cell
Vol. 7, 825-842, May 1996

Specific Interactions of Chromatin with the Nuclear Envelope: Positional Determination within the Nucleus in *Drosophila melanogaster*

Wallace F. Marshall, Abby F. Dernburg, Brian Harmon, David A. Agard, and John W. Sedat*

Department Biochemistry and Biophysics, University of California, San Francisco, San Francisco, California 94143

Submitted December 15, 1995; Accepted February 5, 1996
Monitoring Editor: J. Richard McIntosh

Specific interactions of chromatin with the nuclear envelope (NE) in early embryos of *Drosophila melanogaster* have been mapped and analyzed. Using fluorescence in situ hybridization, the three-dimensional positions of 42 DNA probes, primarily to chromosome 2L, have been mapped in nuclei of intact *Drosophila* embryos, revealing five euchromatic and two heterochromatic regions associated with the NE. These results predict that there are approximately 15 NE contacts per chromosome arm, which delimit large chromatin loops of approximately 1-2 Mb. These NE association sites do not strictly correlate with scaffold-attachment regions, heterochromatin, or binding sites of known chromatin proteins. Pairs of neighboring probes surrounding one NE association site were used to delimit the NE association site more precisely, suggesting that peripheral localization of a large stretch of chromatin is likely to result from NE association at a single discrete site. These NE interactions are not established until after telophase, by which time the nuclear envelope has reassembled around the chromosomes, and they are thus unlikely to be involved in binding of NE vesicles to chromosomes following mitosis. Analysis of positions of these probes also reveals that the interphase nucleus is strongly polarized in a Rabl configuration which, together with specific targeting to the NE or to the nuclear interior, results in each locus occupying a highly determined position within the nucleus.

INTRODUCTION

Studies of nuclear organization suggest that the eukaryotic nucleus is not simply a bag of DNA but rather a highly structured organelle. For example, individual chromosomes and chromosome domains occupy well-defined territories within the nucleus, and in many cases the chromosomes assume characteristic configurations or positions (Comings, 1980; Mathog *et al.*, 1984; Hilliker and Appels, 1989; Cremer *et al.* 1993; Spector, 1993). If chromatin was unconstrained and free to diffuse at random, such nuclear organization could not be maintained. The persistence of a defined arrangement of chromosomes within the nucleus is thus likely to require interactions between chromosome domains and some other nuclear component that would serve as a scaffold or anchor. The most obvious structure to which chromosomes can be anchored is the nuclear envelope, and chromatin-NE interactions are thus likely to play a major role in nuclear organization.

Associations between chromatin and the nuclear envelope (NE) have been observed cytologically for many years (DuPraw, 1965; Murray and Davies, 1979; Quick, 1980; Hochstrasser *et al.*, 1986; Loidl, 1990; Paddy *et al.*, 1990; Belmont *et al.*, 1993). It has been proposed that these chromatin-NE interactions may play a role in a variety of processes, including organization of the interphase nucleus (Comings, 1980), gene regulation (Blobel, 1985; Hutchison and Weintraub,

* Corresponding author.

1985; Palladino *et al.* 1993), chromatin condensation (Hiraoka, 1989), nuclear reassembly (reviewed in Wiese and Wilson, 1993), and meiotic homologue pairing (reviewed in Loidl, 1990). However with the exception of meiotic telomeres (Loidl, 1990; Dernburg *et al.*, 1995), it is not known which loci interact with the NE, particularly during interphase. Indeed, it is not known for certain if the interphase chromatin-NE contacts observed in the microscope involve NE-binding by specific chromosomal loci, a general association of chromatin with the NE, or merely coincidental contact. If chromatin-NE interactions are site specific, then a knowledge of precisely which sites associate with the NE in interphase could shed light on the role of such interactions in the nucleus. In addition, a map of NE-associated sites would facilitate identification of the molecular determinants of the interaction, and provide a basis for comparing cell-cycle dependent or developmental changes in NE association. Furthermore, such a map of NE interactions would allow manipulation, via chromosome rearrangements, of the pattern of NE contacts to test for possible functions.

One possible way to find NE-binding sites is to isolate DNA that binds to the nuclear scaffold or matrix. The nuclear scaffold is operationally defined as the insoluble fraction resulting from extraction of isolated nuclei to remove most of the chromatin (Berezney and Coffey, 1974). Specific DNA sequences, called scaffold attachment regions (SARs), coprecipitate with the scaffold after restriction endonuclease digestions, and bind the nuclear scaffold in vitro (Gasser and Laemmli, 1986). Because lamins are major components of nuclear scaffolds (Lebkowski and Laemmli, 1982), and in light of claims that a *Drosophila* SAR can bind directly to nuclear lamins (Luderus *et al.*, 1992), it is possible that some SARs may bind the NE in vivo. However, *Drosophila* SARs have been shown by others to bind in vitro to the internal rather than the peripheral lamin-enriched component of the scaffold (Izaurralde *et al.*, 1988). The binding of SARs to the nuclear envelope is thus a controversial question. Moreover, the relevance of the various nuclear scaffold preparations to actual nuclear structures in vivo is itself a matter of some controversy (Jackson *et al.*, 1990).

In addition to SAR preparations, in vitro binding studies using defined components have identified proteins that may be involved in chromatin-NE interactions (Glass and Gerace, 1990; Worman *et al.*, 1990; Yuan *et al.* 1991; Foisner and Gerace, 1993; Glass *et al.*, 1993; Sukegawa and Blobel, 1993; Luderus *et al.*, 1994). However, without knowing which chromosomal loci interact with the NE in intact nuclei, these results may be difficult to interpret. Therefore, an alternative method for detecting chromatin-NE interactions in intact cells would be a useful complement to in vitro binding experiments.

One such alternative approach is to use microscopy to visualize the localization of specific chromosomal loci with respect to the NE. In addition to circumventing some of the difficulties inherent in strictly biochemical approaches, visualization of chromatin-NE interactions in the context of the intact nucleus will allow further investigations of the relations between these sites and other nuclear structures, such as lamin fibers (Belmont *et al.*, 1993), the nucleolus (Manuelidis and Borden, 1988; Billia and De Boni, 1991), or foci of transcription and replication (Spector, 1993; Hassan *et al.*, 1994). Furthermore, a microscopic approach is readily applied to a wide variety of tissues, and even to multiple cell types within a single tissue, facilitating an analysis of developmental, cell-cycle, or tissue-specific changes in the pattern of NE contact.

Several groups have employed three-dimensional microscopy to ask whether or not particular genomic loci localize to the nuclear envelope in interphase nuclei. It is not sufficient merely to examine images and visually observe peripheral localization, because within a sphere, the majority of randomly localized points will fall near the periphery. Therefore, it is necessary to demonstrate that peripheral localization is significantly greater than that expected at random. One method is to show that some loci lie on the nuclear surface more often than others (Manuelidis and Borden, 1988). Other groups have carried out a statistical analysis employing a theoretical model for the distribution of points within a nucleus, which is computed either analytically (Chung *et al.*, 1990; Ferguson and Ward, 1992; Vourc'h *et al.* 1993) or using a Monte Carlo method (Van Dekken *et al.*, 1990; Hoefers *et al.*, 1993). Using these methods, localization of centromeres and telomeres with respect to the NE has been analyzed, but the NE association of euchromatic loci in general has not been specifically addressed.

In this report, we describe a light microscopy–based assay for NE association to identify interactions between specific loci and the nuclear envelope in cycle 13 *Drosophila* embryos. This method has been applied to map the position of a series of probes in the euchromatin of chromosome 2 as well as a number of heterochromatic satellite sequences, revealing a number of specific NE contacts. Comparison of the NE contact sites with known SARs (Gasser and Laemmli, 1986), boundary elements (Udvardy *et al.*, 1985), and intercalary heterochromatin (Zhimulev *et al.*, 1982) suggests that NE association may involve a novel type of DNA element. Remarkably, these data also reveal strong positioning of different loci within the interphase nucleus.

MATERIALS AND METHODS

Preparation of Genomic Fluorescence In Situ Hybridization (FISH) Probes

Our mapping effort takes advantage of a library of genomic clones currently employed by the Berkeley *Drosophila* Genome Project for their large scale mapping and sequencing of whole *Drosophila* chromosomes. Bacteria containing specific P1 genomic clones were provided by Gerald Rubin (University of California, Berkeley, CA). These P1 clones originated from a library developed by Hartl and coworkers (Hartl *et al.*, 1994), who mapped the genomic location of many of the clones by hybridization to polytene chromosomes. All clones used in the experiments described here were previously mapped on polytene chromosomes by Hartl *et al.* (1994). Each P1 contains approximately 80 kb of Drosophila genomic DNA. Use of DNA spanning such a large region has proven to be essential for obtaining high signal-to-noise ratios in the FISH procedure. Two microliters of LB-Kan medium were inoculated with 2 μL of an overnight culture of P1-containing bacteria and grown for 3 h at 37°C. Then 2 μL of 1 M IPTG was added and the culture was grown another 3 h before harvesting cells. P1 DNA was obtained by alkaline lysis miniprep from 1 ml of this culture (Sambrook *et al.*, 1989), and amplified using degenerate oligonucleotide-primed polymerase chain reaction (Telenius *et al.*, 1992). Probe DNA was then digested with 4-base cutting restriction enzymes and end-labeled with rhodamine-4-dUTP (FluoroRed, Amersham, Arlington Heights, IL) using terminal transferase (Ratliff Biochemical, Los Alamos, NM). For double-label experiments, one probe was labeled with rhodamine-4-dUTP (FluoroRed) and the other with fluorescein-dUTP (FluoroGreen, Amersham). Probes were checked by hybridization to polytene chromosome squashes to verify detection of the correct locus. Probes specific for heterochromatic repeats were made directly from cloned satellite DNA or synthetic oligonucleotides, using the same labeling procedure. The Rsp probe was a kind gift of Dr. C.-I. Wu (University of Chicago, IL). Dr. A. Villasante (Centre d'Investigacio i Desenvolupament, Barcelona, Spain) generously provided a cloned dodecasatellite probe.

Fixation, Hybridization, and Staining

Drosophila embryos (Oregon-R) collected from population cages were bleach dechorionated and fixed in 3.7% formaldehyde as described by Paddy *et al.* (1990). Approximately 40 μl packed volume of embryos were then placed in 500-ml Eppendorf tubes for all subsequent steps. In situ hybridization was then carried out using a modification of a published method that preserves the structural integrity of the embryos and chromosomes (Hiraoka *et al.*, 1993). Pretreatment of embryos with RNase has no effect on the resulting images, indicating that FISH signals represent hybridization to DNA (Hiraoka *et al.*, 1993). Following hybridization, embryos were washed four times in 2× SSCT (0.3 M NaCl, 0.03 M Na_3 citrate, 0.1% Tween-20). All subsequent steps were carried out at room temperature. Immunofluorescence was carried out on hybridized embryos with anti-*Drosophila* lamin monoclonal T40 (Paddy *et al.*, 1990) as follows. Embryos were blocked by incubating with 6 mg/ml normal goat serum (Jackson Immunoresearch Laboratories, West Grove, PA) in 2× SSCT for 4 h on a rotating plate mixer. Embryos were then washed three times in 2× SSCT. Embryos were then incubated overnight with T40 ascites fluid diluted 1:40 in 2× SSCT and then washed three times in 2× SSCT for 10 min, 1 h, and 1.5 h. Next, embryos were incubated for 4 h with fluorescein-conjugated goat anti-mouse secondary antibodies (Jackson Immunoresearch Laboratories) at 7 μg/ml in 2× SSCT. For double-label experiments in which FISH probes were labeled with rhodamine and fluorescein, Cy-5–conjugated goat anti-mouse secondary antibodies were employed (Jackson Immunoresearch Laboratories). After incubation with secondary antibodies, embryos were washed twice quickly in 2× SSCT, then once for 3 h and washed overnight. Embryos were then stained with 0.5 μg/ml 4,6,-diamidino-2-phenylindole (DAPI), a DNA-specific stain, in 2× SSCT for 10 min. Finally embryos were washed twice in 50 mM Tris-Cl, pH 8.0, and pipetted onto a glass slide between two #0 coverslip spacers. Buffer was aspirated away, and embryos were overlaid with antifade mounting medium (Vectashield, Vector Laboratories, Burlingame, CA). A #1.5 coverslip was then placed over the embryos and sealed with clear nailpolish. To ensure that all embryos analyzed were at the same developmental stage, only embryos in interphase of the 13th embryonic division cycle (as judged by number of nuclei per field of view) were imaged.

Three-dimensional Wide-field Fluorescence Microscopy

Data collection was carried out using multiwavelength wide-field three-dimensional microscopy (Hiraoka *et al.*, 1991) in which a scientific grade cooled CCD camera is used to acquire images, and in which all shutters, filter wheels, stage motion, and image acquisition are under computer control. Embryos were imaged using a 60 × 1.4 N.A. lens (Olympus) and n = 1.5180 immersion oil (R.P. Cargille Laboratories, Cedar Grove, NJ). Three-dimensional datasets, each containing 40-60 nuclei, were acquired by moving the stage in 0.5-μm intervals. Under these conditions, the pixel size is 0.1117 × 0.1117 μm in the xy plane and 0.5 μm in the z axis. At each focus position, an image was acquired at each of three wavelengths (605 nm, 540 nm, and 460 nm) corresponding to the three fluorophores used (rhodamine, fluorescein, and DAPI). Out of focus light was removed by constrained iterative deconvolution (Agard *et al.*, 1989). Examples of such images are given in Figure 1. NE association of the FISH signals were analyzed based on these images, using the following procedure, which is summarized in Figure 2.

Interactive Location of FISH Signals

An interactive three-dimensional visualization package (Chen *et al.*, 1995) was used to interactively pick the three-dimensional location of FISH signals (Figure 2A). When picking FISH spots, some hybridization signals are seen to consist of two closely adjacent smaller spots, in which case the approximate center of mass of both smaller spots taken together is chosen for the location of the signal. Once the approximate location of a FISH spot is interactively picked, the intensity-weighted center of mass is found in a 5 × 5 × 3 pixel region centered on the manually chosen point. This refined FISH spot location is used for all subsequent analysis.

Detecting and Fitting the Nuclear Surface

Pixels belonging to the NE are automatically extracted by locating local intensity peaks in the lamin image. Local maxima are found within adjacent nonoverlapping 15 × 15 × 5 pixel boxes, and their coordinates recorded. Only local-maxima whose intensity exceeds a user-specified threshold are included in the fit.

Each intensity peak is assigned to a particular nucleus, creating for each nucleus a set of points on the NE to which a surface will be fitted. The approximate center of each nucleus is chosen interactively. All lamin intensity peaks falling within a cylindrical region around each nucleus are assigned to that nucleus. The height (h_{cut}) and radius (r_{cut}) of this cylinder are chosen interactively for each dataset to best match the radius and height of the nuclei (Figure 2B).

Once a set of points has been assigned to each nucleus, a surface is fit to this set of points (Figure 2C). We employ a surface harmonic expansion to represent the surface (Purcell *et al.*, 1991). This representation is simple to calculate, can represent a wide variety of nuclear shapes, and can be fitted to a set of points of arbitrary number, placement, and ordering. The surface harmonic expansion describes the surface in spherical coordinates and takes the form:

$$r(\theta,\phi) = \sum_{n=0}^{N} [a_n P_n(\cos\theta) + \sum_{m=1}^{n} (a_{nm}\cos m\phi + b_{nm}\sin m\phi) P_n^m(\cos\theta)] \quad (1)$$

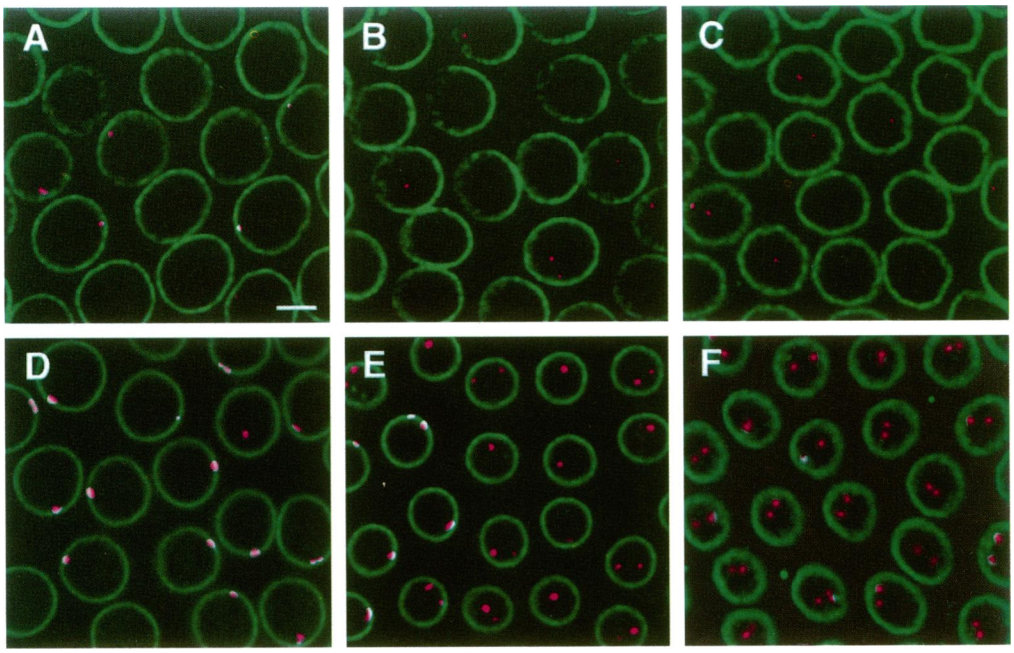

Figure 1. Single optical sections taken from three-dimesional multiwavelength images of cycle 13 embryos. Specific chromosome regions are localized using FISH (in pink) followed by lamin immunofluorescence (in green) to visualize nuclear envelope. In this figure, not all nuclei appear to contain FISH spots because these images are only single optical sections. (A–C) Probes made from P1 clones of euchromatic sequences, (D–F) probes made from heterochromatic satellite sequences. (A) DS03071 is NE associated. (B) DS00861 is randomly localized. (C) DS08107 is nonrandomly far from the NE. (D) AATAC satellite, NE associated. (E) AACAC satellite, randomly localized. (F) Rsp, nonrandomly far from NE. Bar, 4 μm.

where P_n^m are Legendre polynomials, and r is the radial distance from the origin to the surface at the angles θ and ϕ. For nuclei of *Drosophila* embryos, only terms up to N = 4 are included in the expansion.

The surface for a nucleus is found by least-squares fitting the surface harmonic expansion to the set of NE points assigned to that nucleus. The centroid (x_0, y_0, z_0) of the set of NE points is calculated and is used to define the origin of the spherical coordinate system for that nucleus. Next, a set of equations is set up, one for each point to be fit. These are of the form:

$$r_i = r(\theta_i,\phi_i) \tag{2}$$

The unknown parameters to be estimated are a_n, a_{nm}, and b_{nm}, the coefficients of the surface harmonic expansion, which determine the function r( ), and hence the shape of the nucleus, by equation 1. The position of each point (x_i, y_i, z_i) to which the surface will be fitted is converted into spherical coordinates (r_i, θ_i, ϕ_i). Given N_p such points to fit, we seek the coefficients that minimize the quantity:

$$\epsilon^2 = \frac{1}{N_p}\sum_{i=1}^{N_p}[r_i - r(\theta_i,\phi_i)]^2 \tag{3}$$

This linear least squares problem is solved using a singular-value decomposition routine (NAG FORTRAN Library Mark 15, NAG, Downers Grove, IL). As illustrated in Figure 3, the surface generated by this surface harmonic fitting matches the NE shape quite well, and smoothly spans gaps in the lamin signal. When the residual fitting error ϵ defined by equation 3 is averaged for 256 nuclei taken from five randomly chosen datasets, the average fitting error ϵ is 0.28 μm. Because the lamin in these images is approximately 0.5 μm thick (see below), and because points throughout this thick lamin image are used to fit the surface, we expect a residual fitting error on the order of half the thickness of the lamin image, or 0.25 μm, which is close to what is observed. Although a deviation in the surface of 0.28 μm will have some effect on the measured distances to the NE, these effects will be comparable (and to some extent due to) the uncertainty of where the actual surface of the nuclear envelope is within the lamin image.

To compute the distance of a FISH signal to the surface, the position (r_{fish}, θ_{fish}, ϕ_{fish}) of the manually chosen FISH spot is first determined in spherical coordinates. The radial distance from the FISH spot to the surface is then given by the equation:

$$d_r = r(\theta_{fish},\phi_{fish}) - r_{fish} \tag{4}$$

Monte Carlo Analysis

To test for nonrandom association of a FISH signal with the NE, a set of randomly distributed points is generated within each individual nucleus (Figure 2D). The surface defined by equation 1 is used to define a volume within which to generate points. We compensate for the effect of the Rabl orientation by generating random points whose positions are distributed in the z axis with the same distribution as the observed FISH signals. To determine the distribution of z positions due to the Rabl orientation, the vertical offset between each FISH spot and the center of the nucleus is measured. The sample average and variance of these vertical offsets are computed. Then randomly localized points are generated in a system of Cartesian coordinates with origin at the center of the nucleus. The z (vertical) position of each point is a Gaussian-distributed random variable generated by the Box-Muller normal approximation (Press *et al.*, 1989) with mean and variance equal to the sample mean and variance in the vertical position of the observed FISH spots relative to z0. The x and y positions are uniform random variables with range $\pm$ r_{cut} (defined above). For each point thus generated, the radial distance (d_r) to the surface as defined by equation 4 is computed. If $d_r < 0$, the randomly generated point would lie outside the surface and is not to be considered, so that point is discarded and a new point is generated, this process being repeated until a point inside the surface is generated. For telophase nuclei, in which the nuclei are not all oriented the same way, FISH using a dodecasatellite probe was used to detect the centromeric region. A vector from the center of the nucleus to the center of the dodecasatellite signal was taken as the orientation of that nucleus. This vector was then used instead of the z axis to define the vertical

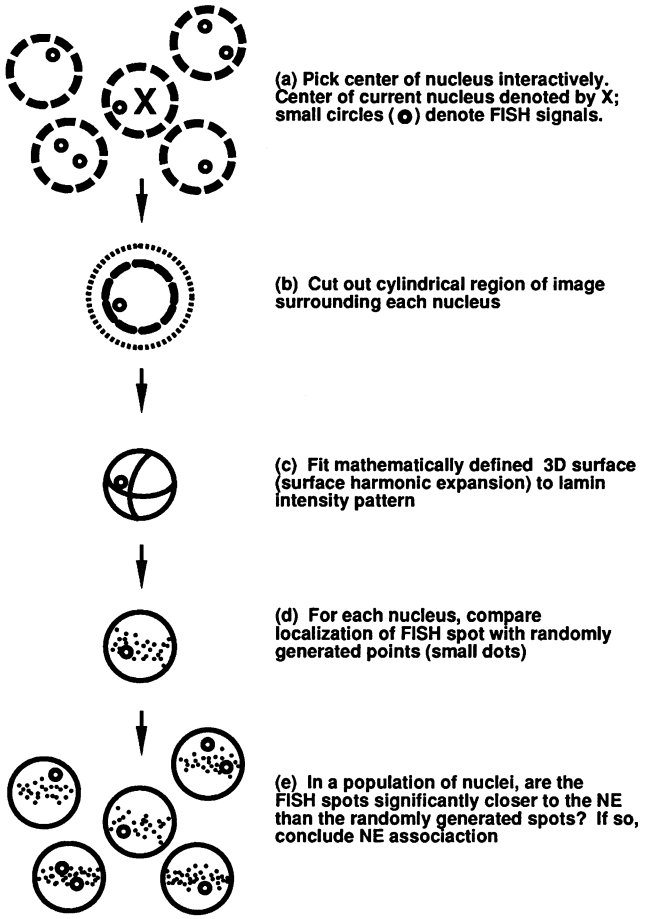

Figure 2. Diagram of image analysis procedure as specified in MATERIALS AND METHODS.

axis for that nucleus, and all calculations of mean vertical position and random point generation were carried out in this frame of reference.

The set of random points is used to determine if a given FISH spot is unusually close to the NE. We define "close" as follows. For a given FISH spot, the above procedure is used to generate 5000 random points within the nucleus. These points are divided into two sets; those that are closer to the NE than the observed FISH spot (Sclose), and those that are farther from the NE (Sfar). To compensate for nonuniform distribution of bulk chromatin within the nucleus (Chung *et al.*, 1990), the DAPI intensity at each point in each set is summed (yielding the sums Dclose and Dfar, respectively). A ratio is then computed using the equation:

$$\rho = \frac{\text{Dclose}}{\text{Dclose} + \text{Dfar}} \tag{5}$$

Note that ρ represents the fraction of chromatin that is closer to the NE than the observed FISH signal. If $\rho < 0.5$ then the FISH spot is declared "peripheral," because less than half of the chromatin is closer to the NE than the FISH spot. If $\rho > 0.5$ the FISH spot is classified as being "internal" from the NE, because more than half of the chromatin is closer. By this definition, without interaction with the NE, a random locus should be classified as peripheral approximately 50% of the time. Therefore a test is necessary to determine if in a large population of FISH points, the frequency of peripheral points is significantly greater than 50% (Figure 2E). Note that classification of points as peripheral if they are closer to the NE than 50% of chromatin is arbitrary. As discussed below, if peripheral is redefined to include only those FISH spots closer to the NE than 80% of chromatin, the results of the analysis for the probes examined here is essentially the same. The reason that the choice of percentile for defining peripheral is not critical is that the statistical test takes this value into account, and simply looks for deviations from the expected frequency of a point being peripheral. Attachment to the NE in some fraction of nuclei will cause a nonrandomly large number of FISH signals to be located near the periphery and will thus produce a deviation in the frequency of peripheral spots no matter what percent of chromatin is chosen for the definition. We note that the test is based on looking for subtle deviations in distribution, rather than simply scoring the frequency of actual NE contact, to increase the sensitivity of the search: FISH probes hybridizing to regions near, but not actually containing, an NE binding site will probably not be localized exactly on the NE, but their distribution will still be biased to a more peripheral distribution.

Assume that there are total of n FISH spots, out of which c are classified as peripheral, and that the expected frequency of peripheral spots (under the hypothesis that the locus is not interacting with the NE and hence is distributed the same as a randomly chosen point) is p, where p = 0.5 according to the above definition (note that, as observed above, other values for the expected frequency p can be used, in which case a different ρ would be taken as the cutoff for the definition of peripheral). The null hypothesis we wish to test is that the frequency of peripheral points is the same as that pre-

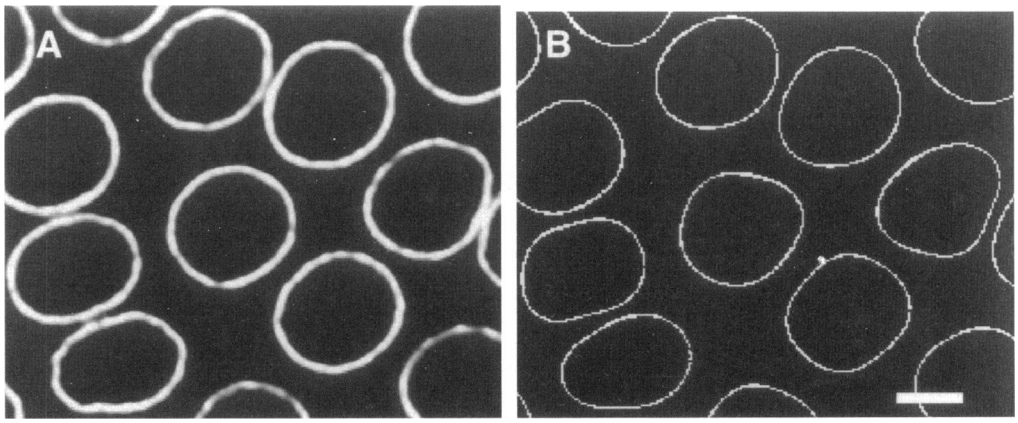

Figure 3. Fitting of NE using surface harmonic expansion fit to lamin signal. (A) Single optical section through three-dimensional lamin image. (B) Surface harmonic expansions for the nuclear surfaces in panel A, plotted in the corresponding plane only. Notice that the lamin signal is punctate and that the nucleus is not, in general, ellipsoidal. As illustrated in panel B, the surface harmonic expansion fits a smooth closed surface to such irregular shapes. Bar, 4 μm.

dicted for random points. We seek a critical value k* that is the maximum number of peripheral spots that we expect if the locus is in fact randomly localized with respect to the NE. Then if $c > k^*$, we would reject the hypothesis of randomness. For a significance level of α the critical value k* can be expressed as:

$$k^* = np + 0.5 + Z_{1-\alpha}\sqrt{npq} \quad (6)$$

where $Z_{1-\alpha}$ is the 1-α-percentile of the standard normal, and $q = 1 - p$. Equation 6 is the standard method for comparison of an observed frequency with an expected frequency given by p (Papoulis, 1990). The critical value is determined by choosing $\alpha = 0.001$. Thus, if for a given FISH probe, more than k* out of n spots are classified as peripheral we reject the hypothesis of randomness with $p < 0.001$, and conclude that the locus in question is associated with the nuclear envelope. Loci for which the hypothesis of randomness has been rejected will henceforth be referred to as close.

If we consider the fraction of points classified as internal relative to the NE, it is possible to formulate a similar test to detect loci that are nonrandomly targeted to the nuclear interior. In this case, the same statistical test applies, except that in this case if more than k* out of n spots are internal, we conclude a nonrandomly interior localization. Such regions will henceforth be referred to as "far" from the NE. Loci that are classified as neither close nor far will be classified as "random," because their localization cannot be distinguished from that of a random point by this test. We note that although a relatively stringent value of α (0.001) was used in the test, for the loci classified as random in Table 1, the null hypothesis of randomness could not be rejected even when setting $\alpha = 0.01$, a much less stringent test. Thus, the discrepancy between close and random loci was quite large and the danger of false positives is small. As a test of the self-consistency of the algorithm, we used the random-point generation scheme outlined above to generate, in each nucleus of an actual dataset, one or two points (depending on the number of FISH spots observed in the actual data). To bias the choice of random points according to the DAPI intensity distribution, initially 1000 points were generated for each nucleus and their positions, along with the DAPI intensity at that position, stored as records in an array. A random number X was then generated between 0 and the total sum of the DAPI intensities for all 1000 points. The array of points was then traversed in order, and at each new element in the array the DAPI intensity was added to a running sum. When this sum exceeded the random value X, that element of the array was then chosen. In this way, the chance that a particular element of the array would be chosen was proportional to the DAPI intensity at that point. These random points were then fed back into the Monte Carlo test routine, and the test performed. For a dataset of 49 FISH spots, this procedure was carried out five times using a different initialization of the random number generator for each run. The results were a number c of peripheral spots of 17, 26, 24, 22, 26 out of 49. In no case were these numbers significantly different from random. By contrast, the actual FISH data showed a highly significant association with the NE. Thus the algorithm is consistent in that random points generated artificially are indeed classified as random.

As mentioned above, the results presented here do not depend on the choice of p. If $p = 0.2$ is used instead, the result is essentially the same, with the exception that DS00178, DS00277, DS05247, and DS07049, which are classified as close when $p = 0.5$, are classified as random when $p = 0.2$. Note that of these four sites, only one showed a highly significant ($\alpha = 0.001$) association with the NE, and this result only affects the apparent extent of the NE associated regions, not their number or location. Finally, we reiterate that this test is designed to detect sites whose localization is biased toward the NE. This should include sites near but not actually including an NE binding site. The test was designed in this way to allow mapping of NE association sites using coarsely spaced probes, so that a large region of a chromosome can be covered without having to use a contiguous set of probes, and still detect most if not all NE association sites. For this reason, however, we should expect that many loci tested will show a peripheral bias in their localization, without actually touching the NE in the majority of nuclei.

Analysis of Double-label Experiments

Embryos labeled with two different probes in two different colors were analyzed to determine which probe of the pair was closer to the NE. Nuclear surfaces were represented as above, and distances were measured using equation 4. Only pairs of FISH spots for which one or both spots were within 0.3 μm of the NE were used for analysis. Distances to the NE were compared between the two adjacent spots. When tabulating Table 3, pairs of spots for which the difference between the two distances is less than 0.1 μm were counted as being equidistant from the NE, so that only relatively major differences in distance were counted when determining which spot is closer.

RESULTS

Strategy for Detecting NE Association

A novel statistical test for NE association has been developed in which the positions of specific loci are determined by FISH followed by anti-lamin immunofluorescence to visualize the NE (see Figure 1 for examples). The DNA in situ hybridization method employed here has been carefully optimized to preserve large-scale chromosome structure, based on a number of criteria including direct comparison with live chromosome structure (Hiraoka *et al.*, 1993). Following three-dimensional data collection using wide-field fluorescence microscopy, the images are analyzed using the procedure summarized in Figure 2. Nuclei and FISH signals are located within the image and the nuclear surfaces are computationally modeled using the anti-lamin immunofluorescence image data (Figure 3). A large number of randomly localized points are then generated within the nucleus, and the distribution of distances from each point to the surface is computed. This distribution is then compared with the observed distances to the surface to determine if the locus is nonrandomly associated with the NE. This statistical analysis, described in MATERIALS AND METHODS, is unique in that it takes into account the effects of variation in nuclear shape, large-scale chromosome organization, and nonuniform distribution of bulk chromatin, thus representing a significant advance over previous statistical techniques for detecting NE association (van Dekken *et al.*, 1990; Hoefers *et al.*, 1993). Loci that are NE associated will henceforth be referred to as close. Loci for which an NE association is not apparent fall into two classes. One class is localized nonrandomly to the nuclear interior (which will be referred to as far) and the other has a distribution matching that of a random point, and is hence termed random. Formal definitions of close, random, and far are given in MATERIALS AND METHODS.

Table 1. Probes tested for NE association

Probe	Locus	Result	n	c	f_c	d_{av} (μm)	z_{av} (μm)
DS05785	97D1–97D2	Random	35	17	0.51	0.61	0.1
DS03117	90C7–90C8	Random	49	30	0.37	1.0	−0.2
DS04383	87B1–87B2	CLOSE	126	91	0.48	0.8	0.5
DS00189	84A6–84B2	Random	38	20	0.16	1.2	0.6
Histone	39D–39E	FAR	114	9	0.01	2.0	1.8
Histone*	39D–39E	FAR	135	24	0.04	1.8	−0.7
DS08107	39B3–39B3	FAR	50	9	0.06	1.8	1.4
DS00861	35F1–35F2	Random	97	41	0.12	1.4	0.4
DS01406	35E1–35E2	Random	39	17	0.23	1.4	−0.3
DS08880	35C4–35C4	Random	62	31	0.23	1.3	0.3
DS01695	35B3–35B6	CLOSE	215	156	0.42	0.9	0.2
DS03792	35A1–35A2	CLOSE	197	127	0.36	0.9	0.6
DS00889	34F3–34F4	CLOSE	138	94	0.36	1.0	0.2
DS03933	34F2–34F3	CLOSE	82	56	0.51	0.8	0.3
DS05899	34F1–34F2	CLOSE	220	166	0.43	0.8	0.5
DS02809	34F1–34F2	Random	98	51	0.28	1.1	0.5
DS00428	34E4–34E5	Random	32	21	0.47	0.8	0.2
DS03232	34E1–34E2	Random	55	29	0.29	1.2	0.4
DS04191	34D1–34D6	Random	19	10	0.16	1.3	0.8
DS01386	34C4–34D2	Random	47	27	0.28	1.1	0.3
DS00576	34A5–34A11	CLOSE	117	80	0.44	0.8	0.3
DS03455	34A1–34A2	Random	35	24	0.49	0.8	0.0
DS04289	33D4–33E2	Random	24	11	0.29	0.9	−1.3
DS07167	33D3–33D4	CLOSE	68	50	0.49	0.8	−0.1
DS00178	33C1–33C6	CLOSE	128	82	0.38	1.0	0.1
DS06189	33A3–33A8	CLOSE	40	32	0.55	0.7	−0.8
DS02634	32E1–32E2	CLOSE ($p < 0.01$)	37	27	0.41	1.0	−0.2
DS07149	23B2–23C1	Random	43	27	0.37	0.7	−1.4
DS00244	23A1–23A2	CLOSE	52	38	0.58	0.7	−1.5
DS00330	22F1–22F2	Random	29	20	0.48	0.8	−1.1
DS00350	22E1−22E2	Random	77	48	0.48	0.6	−1.5
DS08106	22C1−22C2	Random	63	32	0.37	0.8	−1.6
DS06378	22B3−22B9	CLOSE ($p = 0.01$)	86	54	0.49	0.7	−1.4
DS05247	22A4–22B1	CLOSE ($p = 0.01$)	110	70	0.53	0.7	−1.0
DS00277	22A1−22A2	CLOSE ($p = 0.01$)	78	49	0.55	0.5	−1.5
DS03071	21E3-21E4	CLOSE	76	59	0.72	0.4	−2.1
DS07049	21B2–21B8	CLOSE ($p < 0.01$)	119	74	0.56	0.5	−1.8
rDNA	h20 & h29	CLOSE	131	89	0.26	1.0	0.1
Dodeca	h53	FAR	65	16	0.03	1.4	1.7
AACAC	h45	Random	53	26	0.32	0.9	3.1
AATAC	h6	CLOSE	31	28	0.87	0.3	−0.2
359bp	h31–h32	FAR	32	6	0.00	1.2	1.7
Rsp	h39	FAR	100	9	0.13	1.0	1.9

* Position of histone locus in $lt^{\times 13}$ homozygotes.

Locations of P1 hybridization sites were determined by Hartl *et al.*, (1994). Cytological location of the AACAC satellite is according to I. Zhimulev (personal communication). Locations of all other heterochromatic satellites are according to Lohe *et al.*, (1993).

Abbreviations: number of FISH spots used in analysis (n), number of spots classified as "peripheral" (c), fraction on FISH spots within 0.6 μm of the surface (f_c), average distance from FISH spot to surface (d_{av}), and average vertical position relative to nuclear center of mass (z_{av}).

Detection of Specific Chromatin-NE Interactions

The procedure described above has been applied to a number of loci, primarily on chromosome arm 2L, with results listed in Table 1, and diagrammed schematically in Figures 4. All results presented here were obtained from cycle 13 *Drosophila* embryos. Fourteen of 32 probes to euchromatic loci showed a nonrandomly peripheral localization, which we interpret as indicating an interaction with the NE. Of six heterochromatic loci probed, only two (the AATAC satellite and the rDNA locus) were NE associated, while four (the AACAC satellite, Rsp, dodecasatellite, and the 359bp repeat) were not. Peripheral localization of a particular probe does not necessarily imply that an NE attachment site resides within the region of hybridization, because an NE attachment site near, but not actually inside, the region could be sufficient to recruit the flanking region to the nuclear periphery. For this reason, although clusters of linked probes (for example DS07167, DS00178, DS06189, and DS02634) all

Figure 4. Map of NE association sites for the left arm of chromosome 2 in cycle 13 embryos. Numbered subdivisions given below line. Each numbered subdivision is approximately 1 Mb. Black rectangles below line indicate sites of frequent NE contact in polytene nuclei (Hochstrasser *et al.*, 1986). Localization of specific regions as determined by FISH using P1-derived probes followed by statistical test for NE association (see Table 1) plotted above line: (●), P1 probes hybridizing to NE associated regions; and (○), P1 probes hybridizing to randomly localized regions.

show peripheral localization, the actual attachment site does not necessarily span such a large region. The fact that most attachment sites are detected by several adjacent probes simply reflects the design of the test for NE localization, which, as detailed in MATERIALS AND METHODS, is expected to detect loci near enough to an actual NE binding site to have their localization biased toward the periphery, even if the loci probed are not themselves bound to the NE. In many cases in Table 1, one probe may be strongly NE associated while a neighboring probe has a completely random localization. These drastic differences in localization of neighboring probes is actually not surprising in that the probes used here are spaced roughly 200 kb apart on the genome based on their location on polytene squashes. Although we do not know how genomic distance corresponds to physical distance in *Drosophila*, work in mammalian cells (Yokota *et al.*, 1995) has indicated that loci 100 kb apart are roughly 0.4 μm apart in interphase. Thus, probes 200 kb apart can potentially have quite significant differences in nuclear position. In Table 1 it is apparent that for random probes, approximately 50% of the FISH spots are classified as peripheral. This is due directly to the definition of peripheral spots as those which are closer to the NE than 50% of randomly generated points. For a randomly localized point, this will occur approximately 50% of the time. Thus the result in Table 1 for random points is exactly what we would expect a priori. For most of the probes used here, data were collected from two or more embryos. In all such cases, the results for any one probe are the same in different embryos. Representative probes were tested on different batches of fixed embryos and the results were consistent between batches of embryos.

Direct analysis of NE contact frequencies supports the conclusions of the statistical analysis. In these images, the apparent width of the lamin signal is 0.5 μm and the apparent diameter of the FISH signal is approximately 0.6 μm. These dimensions are significantly greater than the lateral resolution of the microscope (approximately 0.1-0.2 μm) and thus probably represent the actual size of the fluorescent region. Distances used for this analysis are measured from the center of the FISH spot to the center of the lamina, as described by equation 4 in MATERIALS AND METHODS. However, if chromatin on the edge of the FISH spot were to touch the edge of the lamina, the distance between centers would be the sum of the radius of lamina and FISH spot, which is 0.55 μm. Thus, any spot whose center is within approximately 0.55 μm of the center of the lamina is close enough to potentially be in contact with the NE. Table 1 tabulates the frequency with which probes fall within 0.6 μm of the surface, as determined by equation 4. Summing the data in Table 1 for the individual classes of loci, the average frequencies with which a close, random, or far FISH spot is close enough to the NE to be touching it are 0.47, 0.31, and 0.05, respectively, verifying that spots that are NE associated according to the Monte Carlo test are indeed more frequently near the NE than random or far points.

Why do most NE associated sites only contact the NE in a fraction of nuclei? First of all, the statistical test is designed to detect loci near but not actually containing an NE binding site, and such loci are not expected to contact the NE in most nuclei, even if their localization is peripherally biased. Results presented below using a set of neighboring probes in one particular peripheral region will further reinforce this point. Second, as demonstrated below, at the beginning of interphase, most NE-associated sites are randomly arranged within the nucleus, and some time will be required for the chromatin to diffuse to the NE before any interaction is possible. Because interphase in cycle 13 embryos is so short (less than 20 min; see Foe *et al.*, 1993), and diffusion of a large polymer like chromatin is slow, in a significant fraction of nuclei a given NE interaction site will simply not have time to reach the NE, and thus will not be able to make contact with it.

Table 1 also lists the average distance from each probe to the NE. Overall average distances to the NE for the three groups of loci classified as close, random, and far are, respectively, 0.78 $\pm$ 0.2 μm, 1.03 $\pm$ 0.25 μm, and 1.52 $\pm$ 0.41 μm. The differences in these averages are highly significant, with $p < 0.001$. Thus, classification based on the Monte Carlo test reflects statistically significant differences in distance to the NE. Note that the contact frequency and average distance differences do not take into account effects due to differences in nuclear shape or chromatin distribution, thus the fact that the results of the Monte Carlo analysis are mirrored in these simpler comparisons

increases our confidence that the specific details of the Monte Carlo procedure are not leading to erroneous results, and also suggests that the NE associations seen are not so subtle as to be missed by simpler measurements. Note also that the comparison of contact frequencies has been the most frequently applied criterion for NE association used by other workers (Hochstrasser *et al.*, 1986; Manuelidis and Borden, 1988). Differences in contact frequency are also qualitatively evident by direct inspection. Visual inspection (Figure 1) reveals that probes that, by the Monte Carlo test, are NE associated, appear more frequently to contact the NE than randomly localized probes.

Some loci, such as the histone locus or the dodecasatellite (see Table 1) are nonrandomly located in the interior of the nucleus. This localization is statistically highly significant ($p < 0.001$) and is reproducible in different embryos. As indicated in Table 1, both heterochromatic (e.g.. dodecasatellite) and euchromatic (e.g.. histone locus) regions can show this localization pattern.

NE Associations Are Established Later than Telophase

If the NE interactions described here are the remnants of interactions primarily involved in NE reassembly following mitosis, then these sites would have been bound to NE vesicles following anaphase, and should already be NE associated during telophase. FISH and lamin immunofluorescence were carried out, and data collected from telophase nuclei, as shown in Figure 5. All images were acquired from nuclei in which NE assembly was complete but in which nuclei had not yet rotated into their interphase orientation (reviewed in Foe *et al.* 1993). Orientation was determined by carrying out FISH using dodecasatellite probes to localize the centromeric regions, as described in MATERIALS AND METHODS. As listed in Table 2, the NE association pattern in telophase is dramatically different. Loci that are NE associated during interphase are generally not

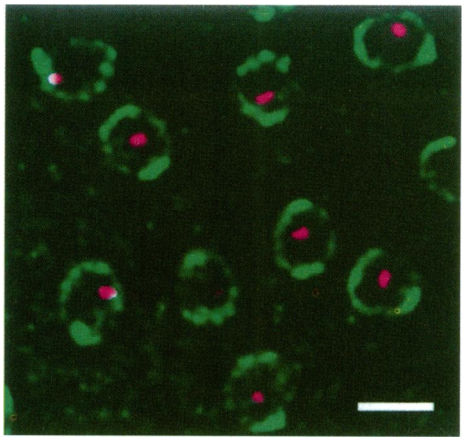

Figure 5. Example of FISH and lamin immunofluorescence in telophase preceding cycle 13. (Pink) FISH signal from AATAC satellite probe; (green) lamin immunofluorescence signal. Bar, 4 μm.

NE associated during telophase, while other loci, such as dodecasatellite itself, appear NE associated in telophase but not in interphase. These changes are reflected in differences in frequency (f_c) of NE contact and average distance (d_{av}) to the NE. The most extreme example is the AATAC satellite that is strongly NE associated in interphase but is in fact nonrandomly far from the NE in telophase. Although the nucleus increases in size between telophase and interphase, the AATAC site actually becomes closer to the NE (d_{av} goes from 0.9 μm to 0.3 μm). Thus, the interphase NE interactions tabulated in Table 1 do not appear to be involved in NE assembly during telophase, but are in fact established later.

Delimiting an NE Binding Region Using Pairs of Probes

Figure 4 indicates that relatively large regions, defined by several adjacent FISH probes, show some degree of NE association. For example, the entire

Table 2. Changes in NE association between telophase and interphase

	Telophase			Interphase		
Probe	Localization	f_c	d_{av} (μm)	Localization	f_c	d_{av} (μm)
DS00861	Random	0.59	0.4	Random	0.12	1.4
DS01695	Random	0.58	0.5	CLOSE	0.42	0.9
DS00576	Random	0.31	0.7	CLOSE	0.44	0.8
AATAC	FAR	0.14	0.9	CLOSE	0.87	0.3
Dodeca	CLOSE	1.0	0.02	FAR	0.03	1.4
Histone	Random	0.65	0.6	FAR	0.01	2.0

Abbreviations: fraction on FISH spots within 0.6 μm of the surface (f_c), and average distance from FISH spot to surface (d_{av}).

region 34F–35B shows a nonrandomly peripheral localization. Based on the size scale of the *Drosophila* cytological map, where one division (e.g. 35) spans approximately 1 Mb, the region from 34F to 35B is roughly 500 kb in size. Does this reflect a general adhesion over a large region, or is there a discrete binding site that recruits flanking chromatin to the periphery? To locate the actual NE interaction site within such a large region, embryos were hybridized simultaneously with pairs of probes, one labeled with fluorescein and one labeled with rhodamine. An image of such an embryo is given in Figure 6A. In each nucleus, the distance from the NE to each FISH spot in each color was measured, allowing us to ask if one spot was consistently closer than another. If one FISH probe hybridizes nearer to, or within, the actual NE binding site, then it will tend to be closer to the NE than a FISH probe hybridizing further away. However, note that because in some nuclei the locus may not actually be bound to the NE but merely coincidentally near the periphery, it is possible for the probe that is farther from the binding site to actually be closer to the NE in some nuclei. For this analysis, only pairs of FISH spots for which at least one spot was within 0.3 μm of the NE were employed, so that only pairs that could be in contact with the NE were scored. The results for four pairs of probes are given in Table 3, and summarized graphically in Figure 6B. It thus appears that probe DS03933 is closer to the NE than any other probe in this region, which is consistent with the frequencies of NE contact tabulated in Table 1. This result suggests that a single NE binding site is in or near the region spanned by DS03933, with the remaining flanking probes recruited to the periphery because they are near to this site on the chromosome.

Polarized Configuration of Interphase Chromosomes

In many cell types, chromosomes are polarized, with telomeres clustered at one end of the nucleus, and centromeres clustered at the other. This polarized configuration is known as the Rabl orientation (reviewed in Comings, 1980). In *Drosophila* embryos all nuclei have the same orientation relative to the embryo surface (Foe and Alberts, 1985; Hiraoka *et al.*, 1990b, 1993), with centromeres grouped outward, on the top of the nucleus nearest to the surface of the embryo, and telomeres pointing inward. When three-dimensional images are collected, all nuclei in the embryo lie in a plane perpendicular to the optical axis (z axis) of the microscope. For each locus, the average vertical position of the FISH signal relative to the center of mass of the nucleus was measured and compared with its genomic location to test for a Rabl chromosome orientation. The vertical position of the FISH signal for given locus is quite consistent, having a standard deviation in the range 0.4 to 0.8 μm, so that within a nucleus approximately 7 μm in height, the loci are constrained to lie within a disk-like region 1- to 2-μm thick. We have listed in Table 1, and plotted in Figure 7, the average vertical positions (z_{av}) of each probe, from which the Rabl orientation is generally evident: loci near the telomere are lower in the nucleus than loci near the centromere.

Different Loci Occupy Defined Positions in the Nucleus

An outstanding question in nuclear organization has been the extent to which a given locus occupies a predetermined position in the nucleus. We can mea-

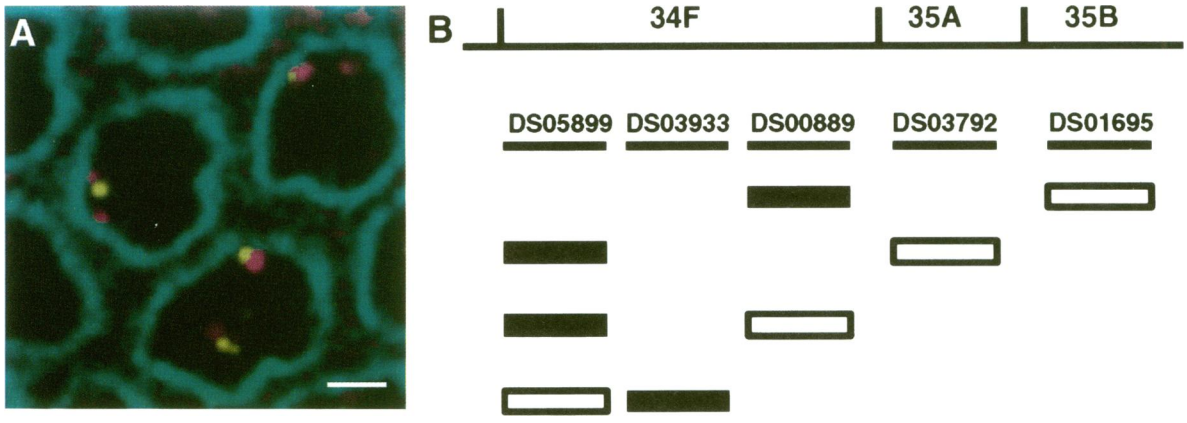

Figure 6. Mapping the NE association site at 34F-35B using pairs of FISH probes labeled in two different colors. (A) Single section from one such double-label dataset, rendered in pseudocolor to visualize lamin fluorescence along with two different FISH colors. (Pink) DS00889 probe labeled with rhodamine, (yellow) DS01695 probe labeled with fluorescein, and (green) anti-lamin staining using Cy-5 conjugated secondary antibodies. Scale bar, 2 μm. (B) Result of double label experiment, as tabulated in Table 3. Probes are aligned to the cytogenetic map at the top of figure. Pairs of rectangles below probes indicate pairs of probes compared. Black rectangles indicate probes that were closer in the majority of nuclei, white rectangles represent probes that were farther.

Table 3. Comparison of distance to NE between pairs of neighboring probes

Red probe	Green probe	$d_R < d_G$	$d_R = d_G$	$d_R > d_G$
DS01695	DS00889	9	4	19
DS00889	DS01695	9	4	4
DS03792	DS05899	12	16	26
DS05899	DS03792	4	2	0
DS05899	DS00889	11	11	6
DS05899	DS03933	4	6	10

Abbreviations: distance measured from the red FISH spot to the NE (d_R), and distance measured from the green FISH spot to the NE (d_G). Columns list number of nuclei in which red spot is closer, equidistant, or farther from the NE than the green spot. See MATERIALS AND METHODS for precise definition of distances. Pairs for which the difference in distance to the NE was less than 0.1 μm were counted as equidistant.

sure position of a FISH spot by two values, the vertical position (z) and the radial distance to the surface (d). These two coordinates are illustrated in Figure 8A, and defined more precisely in MATERIALS AND METHODS. Presumably, the Rabl configuration sets the vertical position of a particular locus, and localization relative to the NE determines the average distance from the locus to the NE, thus setting the radial position. The average values of these two positional coordinates, listed in Table 1, are plotted for several loci in Figure 8B. The striking result of Figure 8B is that different loci do in fact consistently occupy different territories within the nucleus. Furthermore, these coordinates can be specified independently. The position of one site (the histone locus) was analyzed in embryos homozygous for the lt^{x13} translocation (Wakimoto and Hearn, 1990), which translocates the left arm of chromosome 2 to a distal position on the right arm of chromosome 3 (see Figure 8C) with the effect that the histone locus is now shifted to a much more distal position. Figure 8D plots the localization of the histone locus in lt^{x13} as compared with wild type. As expected from its more distal position, and as has been previously demonstrated (Hiraoka *et al.*, 1993), the vertical position of this locus is now more than 2 μm lower in the nucleus, which is what a Rabl configuration would predict. However, the average distance from the locus to the NE is the same as in wild type, indicating that the radial position is unaffected. The breakpoint of lt^{x13} on 3R is located in region 97D, and as shown in Table 1 the 97D region is much closer to the NE than the histone locus. Thus, in lt^{x13} the highly internal radial position was indeed conferred by the histone locus or its flanking regions on 2L, and was not a feature of the adjacent region on 3R.

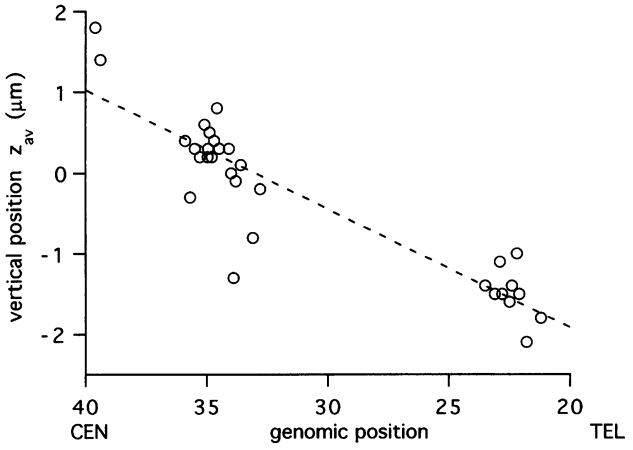

Figure 7. Polarized (Rabl) configuration of chromatin in interphase nucleus. Vertical position taken from Table 1 plotted versus position on chromosome arm 2L, along with best-fit line. Larger values of z_{av} correspond to the end of the nucleus nearest to the surface of the embryo.

DISCUSSION

Distribution of NE Association Sites

Three-dimensional FISH in conjunction with a semi-automated statistical method has been developed to detect specific chromatin-NE associations, and this approach has been used to demonstrate the existence of site-specific chromatin-NE interactions in nuclei in intact cycle 13 *Drosophila* embryos. One important caveat of this work is that in the cycle 13 embryo, zygotic transcription has not yet reached maximum levels, and thus it will be interesting in the future to examine NE interactions in later embryos and adult tissues to determine the effects of transcription and differentiation. Based on these results, in which NE contacts have been mapped along a region covering approximately one-third of chromosome arm 2L, we estimate that there are on the order of 15 NE interaction sites per arm, or a total of 150 NE association sites per diploid nucleus. Note that this value has been extrapolated from a relatively small portion of the genome, and the density of NE contact sites may differ in other regions. These NE-associated sites would be spaced, on average, 1-2 Mb apart, and could thus define the boundaries of large loop domains tethered to the NE in interphase. Evidence for large chromosome loops on the order of 1 Mb in human interphase nuclei has recently been reported (Yokota *et al.*, 1995). We propose that large chromosome loops could be tethered by attachment either to the NE or to an internal structure. Existence of distinct peripheral and internal chromatin anchoring sites has previously been proposed on the basis of in vitro experiments (Lebkowski and Laemmli, 1982). In addition to forming large loops, NE attachment could potentially have direct effects on the

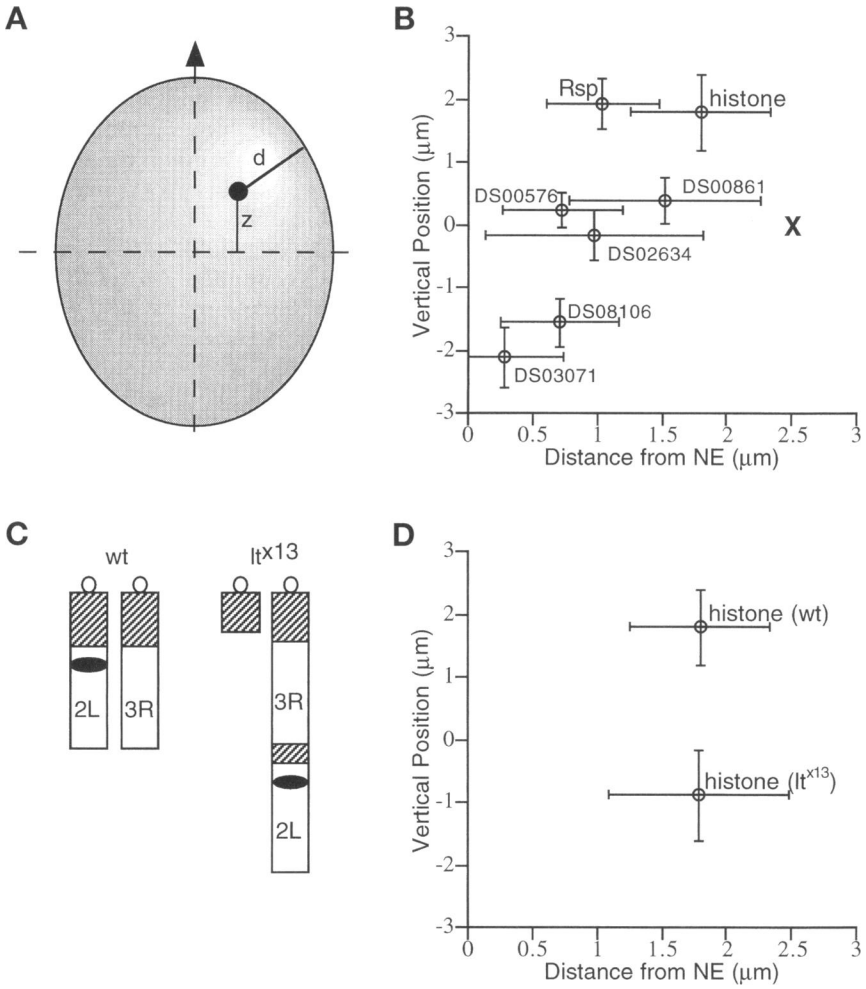

Figure 8. Defined localizations of different loci to specific regions within the nucleus. (A) Position within the nucleus can be described by two coordinates, a vertical height (z) above the center of the nucleus, and a radial distance (d) to the NE, given by equation 4. (B) For each locus, the average vertical position relative to the center of the nucleus is plotted versus the average distance from the NE. Error bars indicate one standard deviation in each measurement. (X) The average position of the center of the nucleus. (C and D) Vertical position and distance from NE specified independently. (D) Diagram of translocation. Chromosome arrangement in wild-type and lt^{x13} translocation; the histone locus is represented by a filled ellipse; hatched and open boxes represent heterochromatin and euchromatin, respectively; the open circle represents the centromere. (D) The localization of the histone locus is plotted as in panel B for wild-type embryos and for embryos homozygous for the lt^{x13} translocation. Shifting histone locus to a more distal position alters vertical position without affecting radial position.

NE-associated loci. It is apparent in Figure 4 and from the results given in Figure 6B that a large region (100-500 kb, assuming 1 Mb per division) flanking each interaction site can be brought to the periphery by a relatively discrete NE association site, so that NE binding at one site could influence the subnuclear localization of a relatively large flanking region. An NE binding site can thus exert an influence on surrounding DNA by targeting it to the NE.

Only a fraction of heterochromatin is associated with the NE in these nuclei. This is in contrast with a common assumption that all heterochromatin is NE associated, and suggests that specific DNA sequences, rather than the heterochromatic state in general, are required to confer NE attachment to heterochromatin. It is, however, probable that in the cycle 13 embryo, the heterochromatic state is not yet fully established (Hiraoka *et al.*, 1993). Comparative studies of NE association in cycle 14 embryos and more developmentally advanced tissues should resolve this issue.

Some regions (the histone locus, dodecasatellite, and Rsp) are not only not associated with the NE, but are in fact nonrandomly far from the NE. This type of localization has been previously described in other cell types (Lawrence *et al.*, 1988; Hoefers *et al.*, 1993; Vourc'h *et al.*, 1993), and may reflect an association with an internal matrix or scaffold. This implies that the nucleus may contain at least two types of subnuclear neighborhoods, a peripheral NE-associated neighborhood, and an internal, possibly matrix-associated, neighborhood.

Other loci are classified as randomly localized. However, this is based solely on distance to the NE, and does not imply that the loci occupy completely random positions in the nucleus with respect to other criteria. Indeed, with respect to vertical positioning (the Rabl orientation) the localization of these loci is clearly nonrandom.

Having identified several NE-associated loci, it should now be possible to test their effects by inserting

reporter genes into these regions, or using chromosome rearrangements to alter the pattern of attachment. Furthermore, the door is now open for a directed search for the molecular components of these interactions. In particular, the method illustrated in Figure 6 of comparing the localization of pairs of nearby probes should allow specific NE binding sites to be pinpointed more precisely. The probes used in Figure 6B fall in a region spanned by a contiguous set of overlapping P1 genomic clones (Berkeley *Drosophila* Genome Project, personal communication), which should allow us, in the near future, to map the NE binding site to within a single P1 clone. Such experiments are currently underway.

Comparison with Previous Studies of Nuclear Organization

Three dimensional reconstructions of polytene nuclei from *Drosophila* salivary glands (Hochstrasser *et al.*, 1986) revealed a number of loci that were found near the NE with an unusually high frequency. These frequent NE contacts were observed at the same loci in other polytenized tissues (Hochstrasser and Sedat, 1987), suggesting that they may be a general feature of nuclear organization. The presence of sites with relatively high frequency of peripheral localization relative to other sites could, however, reflect either an NE association of the former sites or a nonrandomly internal localization of the latter sites. In those studies, four significant NE contact sites were observed on chromosome 2L, at regions 22A-B, 32F-33A, 34F-35C, and 36C-E (Hochstrasser *et al.*, 1986). Figure 4 reveals that of the three regions tested so far (22A-B, 32F-33A, and 34F-35C) all three regions are also associated with the NE in the embryo, suggesting that these interactions can be maintained over long developmental times, and further implying that the high frequency surface contacts seen in the polytene nuclei are indeed due to NE associations. However, several regions that are associated with the NE in the embryo, such as 23A, 34A, and 87B, are not in particularly frequent contact with the NE in polytene nuclei (Hochstrasser *et al.*, 1986), suggesting that these associations may be lost during polytenization. This is consistent with studies of NE-chromosome contact in polytene chromosomes of *Chironomus* and *Acricotopus* (Quick, 1980) in which a progressive loss of NE contact was found to accompany polytenization.

Telomere-NE interactions have been proposed to play a role in meiosis (Loidl, 1990) and telomeric silencing (Palladino *et al.*, 1993). Peripheral localization of telomeres during interphase has previously been reported (Manuelidis and Borden, 1988; van Dekken *et al.*, 1989; Chung *et al.*, 1990) whereas in other cell types telomeres are more internally located (Ferguson and Ward, 1992). Although we have not used telomeric probes in this study due to difficulties with secondary hybridization to nontelomeric sites, the most distal probe employed thus far, DS07049, is indeed associated with the NE. This is in agreement with the observation that during prophase in the *Drosophila* embryo, telomeres often appear to be in contact with the NE (Hiraoka *et al.*, 1990a).

In contrast to telomeres, centromeres are almost certainly not NE associated in the *Drosophila* embryo. Cytological and genetic studies have indicated that the heterochromatic Rsp and dodecasatellite blocks are closely linked to the centromeres of chromosomes 2 and 3, respectively (Wu *et al.* 1988; Pimpinelli and Dimitri, 1989; Carmena *et al.*, 1993). Figure 4 reveals that both Rsp and dodecasatellite are, in fact, nonrandomly far from the NE, implying that centromeres are not NE associated, and may interact with an internal nuclear structure. Such a nonrandomly internal localization of centromeres has previously been reported in vertebrate cells (Hoefers *et al.*, 1993; Zalensky *et al.*, 1995) although other groups have reported peripheral localization of centromeres (Manuelidis and Borden, 1988; van Dekken *et al.*, 1989, 1990; Ferguson and Ward, 1992; Vourc'h *et al.*, 1993).

Relation to SARs and Other Known Chromosomal Elements

Scaffold attachment regions have been described in *Drosophila* embryos (Gasser and Laemmli, 1986). As discussed above, SARs were potential candidates for NE association sites. Four regions containing known SARs were probed in the present work. Of these, two, the Adh (35B3) and hsp-70 (87A7) loci, were indeed within NE-associated regions (see Table 1). However, another SAR, contained in the ftz locus (84B1), was in a randomly localized region, while a fourth, the histone locus (39D-E), was in fact nonrandomly far from the surface. This last result is particularly interesting in light of claims that naked DNA containing the *Drosophila* histone SAR can specifically bind lamin paracrystals in vitro (Luderus *et al.*, 1992, 1994). It has, however, previously been demonstrated that while *Drosophila* SAR DNA can bind nuclear scaffolds in vitro, if scaffolds are prepared that are highly enriched for lamins, and lacking the internal protein network usually seen in other scaffold preparations (Lebkowski and Laemmli, 1982), SAR DNA no longer binds (Izaurralde *et al.*, 1988). The inability of SAR DNA to bind the NE-associated scaffold component in vitro is consistent with our data from intact cells, and implies that SARs do not confer NE association either in vitro or in vivo. In the two cases where a SAR is found in an NE-associated region, there is no evidence that the SAR sequence itself is required for NE association.

One role of NE-associated chromatin could be to form boundaries between independent chromatin do-

mains. A class of loci, known as scs (specialized chromatin structure) elements, has been described that may act as boundaries between chromatin domains (Udvardy *et al.*, 1988; Kellum and Schedl, 1992). Genes flanked by scs elements are insulated from euchromatic position effect and from the action of upstream enhancers, suggesting that these sites function as boundaries of chromatin domains, perhaps by anchoring chromatin to the NE to form topologically independent loops. Although one scs-containing locus, hsp-70 (87A7), is in an NE-associated region, another, the 90BC tRNA locus, located at position 90B-C, is not. Thus there is no strict correlation between NE-associated sites and scs-like elements. We further note that although topologically independent loop domains have been observed in *Drosophila* (Benyajati and Worcel, 1976) they are only 85 kb in length, on average, far smaller than the 1-2 Mb loops defined by the NE associations described here.

Genetic studies have led to the discovery of many chromosomal proteins that are thought to influence chromatin structure and activity. If NE binding requires particular chromosomal proteins, it is possible that genetic identification of such proteins may eventually reveal the proteins involved in NE association. In *Drosophila*, the binding sites of many chromatin proteins have been determined, revealing a limited number of regions on each chromosome that bind different chromatin proteins. However, NE associations do not appear to correlate strictly with any of these binding sites. For example, the 23A NE-associated region contains binding sites for Su(z)2, Psc, and z, but not ph, Pc, or HP-1, while the 33B NE-associated region contains binding sites for ph and Pc, but not Su(z)2, Psc, z, or HP-1 (James *et al.*, 1989; Rastelli *et al.*, 1993). Therefore, NE association does not appear to require binding sites for z, Su(z)2, Psc, ph, Pc, or HP-1.

Finally, NE association sites were compared with the locations of intercalary heterochromatin (IH). Intercalary heterochromatin (Zhimulev *et al.*, 1982) refers to a set of loci found in the euchromatic arms of *Drosophila* polytene chromosomes, which share several characteristics suggestive of a heterochromatic state, including late replication, high frequency of chromosome breaks, and formation of ectopic fibers. On 2L, IH is found in regions 22A, 25A, 25E-F, 33A-B, 34E-35A, 35C-F, 36D, and 39E, as judged primarily by frequency of ectopic fiber formation (Zhimulev *et al.*, 1982). As seen in Table 1, three of these IH-containing regions coincide with NE-associated regions, while one, 39E, is in a region that is nonrandomly far from the NE. Thus, although many IH regions are NE associated in embryos, some are not. In addition, it is clear that some NE-associated regions (for example 34A or 87B) are clearly not IH by any criterion. Thus, IH is neither strictly necessary nor sufficient for NE association. However, IH has been cytologically defined only in polytene nuclei, and it is possible that the exact distribution of regions with IH properties is different in diploid interphase nuclei. In spite of these differences, the fact that three of the most significant IH sites on 2L (Zhimulev *et al.*, 1982) correspond exactly to NE associations seen there is suggestive of some underlying relation between IH and NE association. This is also supported by the fact that essentially all polytene NE contact sites (see above) correspond to IH regions (Hochstrasser *et al.*, 1986).

Relation to Lamin-fiber–associated Chromatin

In vitro binding studies have suggested that lamins may bind chromatin, either directly (Glass and Gerace, 1990; Yuan *et al.*, 1991; Luderus *et al.*, 1992, 1994; Glass *et al.*, 1993) or via lamin-associated proteins (Foisner and Gerace, 1993). Interactions of specific loci with nuclear lamins could be the basis for the associations observed here. The nuclear lamina in *Drosophila* embryos appears in the light microscope to consist of a reticular basketlike structure composed of large fibers (Paddy *et al.*, 1990). Previous studies have revealed that approximately 20-30 chromosomal sites, as detected by DAPI staining, are close enough to one of these large lamin fibers to potentially be in contact with it (Paddy *et al.*, 1990). Although the number (20-30) of such sites is significantly less than the number of specific NE-associated sites reported here, it is possible that a fraction of the NE-associated sites do indeed bind to the regions of heavy lamin staining, while the remainder interact with more diffusely organized lamins, or with some other NE components, such as nuclear pore complexes. In support of this latter possibility, some nuclear pore components contain DNA binding motifs (Sukegawa and Blobel, 1993).

Alternative Models for Apparent NE Association

This work is based on the assumption that the FISH procedure employed does not strongly affect the position of chromatin within the nucleus. Comparison of hybridized chromosomes with both living and fixed nonhybridized chromosomes does not indicate any significant rearrangement due to the FISH procedure (Hiraoka *et al.*, 1993). The minor structural differences between hybridized and unhybridized chromatin are likely to be significant only at much higher resolution than currently available in the light microscope, and should not affect the statistical test employed, which tests for an overall bias in localization rather than actual contact with the NE, and is thus only affected by relatively large displacements. The precise vertical positioning reported here is also not consistent with a scrambling of nuclear organization following hybridization. Ultimately, however, analysis of nuclear orga-

nization in living cells will be required to completely settle this point.

We have tacitly assumed that the strongly peripheral localization observed is due to an interaction of chromatin with the NE. Although this interpretation is the simplest, and is consistent with a significant body of literature supporting the existence of such interactions, nevertheless several alternate models must be considered.

First, since we know that some sites are nonrandomly localized to the nuclear interior, it is possible that the remaining chromosome regions could become peripheral due to either excluded volume effects or rigid loops extending outward. If such a large fraction of the inner 50% of the nucleus was occupied by internal sites as to produce the strong peripheral localizations seen here, then all other sites, not just some, should appear nonrandomly peripheral. This is obviously not the case, as many sites appear randomly localized. Moreover, an excluded volume effect would not explain why only certain loci appear consistently peripheral.

A second possibility is that extended loops may run outward from internally anchored points, thus directing some loci to a peripheral location. This model requires the existence of internal anchor points between any two peripheral sites. Such internal anchor regions should appear nonrandomly far from the NE. However, as seen in Table 1, far points do not in general occur between peripheral sites. Thus, peripheral localization is unlikely to be a consequence of internal localization of other sites, either by excluded volume or rigid loops.

Finally, it remains a formal possibility that the peripheral sites are associated, not with the NE per se, but with some unknown peripheral structure that may or may not be anchored to the NE. With regards to the role these interactions may play in nuclear organization and chromosome dynamics, the nature of the peripheral structure to which they are attached may be less important, and in any event, this question will certainly be resolved once the molecular determinants of the interactions described here are identified.

Interphase NE Interactions Are Not Remnants of NE Reassembly

One interesting function for chromatin-NE interaction would be to mediate NE reassembly following mitosis by binding NE vesicles to anaphase chromosomes. If such binding interactions were to persist until interphase, then at telophase, when the NE has reassembled, the interactions should already be established, which as seen in Table 2, is not the case. Therefore, the specific interactions seen between chromatin and the NE in interphase are not the same as the interactions that bind NE vesicles to chromosomes following mitosis.

Rabl Orientation in Interphase

The Rabl orientation, with centromeres at one end of the nucleus and telomeres at the other (reviewed in Comings, 1980), is evident in *Drosophila* embryos during prophase (Hiraoka *et al.*, 1990a) and following anoxia-induced premature chromosome condensation (Foe and Alberts, 1985). In interphase, FISH has revealed that subtelomeric sequences are located near the bottom of the nucleus facing the embryo interior (Hiraoka *et al.*, 1990b). Furthermore, Hoechst staining in interphase reveals brightly fluorescing heterochromatic blocks located near the top of the nucleus in *Drosophila virilis* embryos (Ellison and Howard, 1981). However, the extent to which the chromosome arms themselves follow this arrangement along their entire length is unknown. In salivary nuclei the path of the chromosomes is not particularly straight, and often loops back before eventually reaching the other side of the nucleus (Hochstrasser *et al.*, 1986). Diploid interphase chromosomes are more flexible than polytene chromosomes, and might be expected a priori to follow an even more meandering path through the nucleus. FISH studies of the histone locus (Hiraoka *et al.*, 1993) revealed it to be constrained to a defined vertical region. As described above, this holds true for all loci investigated here, with each locus lying in an approximately 1 μm wide vertical position defined relative to the center of the nucleus (see Figure 8B). Moreover, as listed in Table 1, and plotted in Figure 7, the average vertical position is correlated with genome position exactly as expected from a Rabl configuration. Loci near the centromere are found near the top of the nucleus, while loci near the telomere are near the bottom of the nucleus. Apparent exceptions to this rule (such as DS00889 versus DS02809) are for the most part minor differences between nearby loci, and are probably due to embryo to embryo variation in nuclear size. However, we cannot rule out, from this study, the possibility of deviations from the strict Rabl configuration due to chromosome arms looping back within the nucleus. It is clear that in addition to the clustering of telomeres and centromeres at opposite ends of the nucleus, other loci on the chromosome arm are similarly constrained according to the general polarization of the nucleus. This high degree of constraint is likely to require anchoring of chromosomes to a rigid structure of some sort, and the NE interactions reported here could serve such a role.

Positional Determination of Chromosomal Loci within the Interphase Nucleus

An important result of this study is that different loci reproducibly occupy defined regions of the nucleus, as detailed in Figure 8B. This is true even for loci not associated with the NE. Some aspects of this positioning are maintained in a translocation (Figure 8D). Furthermore, even loci classified as random with respect to NE association appear to have a specific nuclear sublocalization on the vertical axis and possibly also the radial axis, consistent with the idea that as the chromosome loops in from the NE, loci along the loop occupy preferred radial positions. The size of the error bars could reflect variation in nuclear size, cell cycle-dependent or developmental changes (including apoptosis), or interphase chromosome motion.

Specific positioning within the nucleus could have a strong effect on processes such as transvection or recombination that involve physical interactions between loci, because loci in two completely disparate regions would not be able to interact. The data in Figure 8D demonstrate that it is possible to use chromosome rearrangements to alter the nuclear position of a particular locus. By manipulating nuclear organization in this manner, it should be possible to test whether or not this defined nuclear positioning plays a functional role. The data in Figure 8D also imply that vertical positioning is determined primarily by location within the genome, in accordance with the Rabl configuration, while radial distance to the NE is a more local property of a particular region. This is consistent with the result that NE associations are established after chromosome decondensation in telophase.

This is, to our knowledge, the first clear evidence for specific positioning of multiple different euchromatic loci within the interphase nucleus. Prior studies of three-dimensional nuclear organization (Manuelidis and Borden, 1988; Van Dekken *et al.*, 1990; Ferguson and Ward, 1992; Hoefers *et al.*, 1993; Vourc'h *et al.*, 1993) have focused on only one or two, generally heterochromatic, loci such as centromeres or telomeres. It is likely that a more extensive analysis of the localization of a large number of sites would reveal a similar degree of positioning as that seen here. The *Drosophila* embryo proved particularly well suited to these studies, however, because all nuclei in one dataset are highly synchronized and oriented the same way relative to the surface of the embryo, which allowed a vertical axis to be defined. We predict that in the future, the radial and vertical positioning demonstrated here will turn out to be a general feature of nuclear organization in other cell types. The functional significance of such positioning now remains to be determined.

ACKNOWLEDGMENTS

The authors thank Dr. H. Bass, J. Fung, Dr. M. Gustafsson, and S. Parmelee for critical reading of the manuscript. The statistical test was suggested by Dr. C.W. Marshall, Department of Mathematics, Polytechnic University, Farmingdale, NY. We also acknowledge Gina Dailey and Dr. Gerald Rubin, University of California, Berkeley, CA, for providing P1 genomic clones. This work was supported by a Howard Hughes Medical Institute Predoctoral Fellowship (W.F.M.), National Institutes of Health grants R01-GM-225101-16 and R01-GM-331627-12 (J.W.S. and D.A.A., respectively), and stages of this work were supported by the Howard Hughes Medical Institute (D.A.A. and J.W.S.). D.A.A. is currently an investigator of the Howard Hughes Medical Institute.

REFERENCES

Agard, D.A., Hiraoka, Y., Shaw, P., and Sedat, J.W. (1989). Fluorescence microscopy in three dimensions. Methods Cell Biol. *30*, 353-378.

Belmont, A.S., Zhai, Y., and Thilenius, A. (1993). Lamin B distribution and association with peripheral chromatin revealed by optical sectioning and electron microscopy tomography. J. Cell Biol. *123*, 1671-1685.

Benyajati, C., and Worcel, A. (1976). Isolation, characterization, and structure of the folded interphase genome of *Drosophila melanogaster*. Cell *9*, 393-407.

Berezney, R., and Coffey, D. (1974). Identification of a nuclear protein matrix. Biochem. Biophys. Res. Commun. *60*, 1410-1419.

Billia, F., and De Boni, U. (1991). Localization of centromeric satellite and telomeric DNA sequences in dorsal root ganglion neurons, in vitro. J. Cell Sci. *100*, 219-226.

Blobel, G. (1985). Gene gating: a hypothesis. Proc. Natl. Acad. Sci. USA *82*, 8527-8529.

Carmena, M., Abad, J.P., Villasante, A., and Gonzalez, C. (1993). The *Drosophila melanogaster* dodecasatellite sequence is closely linked to the centromere and can form connections between sister chromatids during mitosis. J. Cell Sci. *105*, 41-50.

Chen, H., Swedlow, J.R., Grote, M., Sedat, J.W., and Agard, D.A. (1995). The collection, processing, and display of digital three-dimensional images of biological specimens. In: Handbook of Biological Confocal Microscopy, ed. J.B. Pawley, New York: Plenum, 197-210.

Chung, H.M., Shea, C., Fields, S., Taub, R.N., Van der Ploeg, L.H.T., and Tse, D.B. (1990). Architectural organization in the interphase nucleus of the protozoan *Trypanosoma brucei*: location of telomeres and mini-chromosomes. EMBO J. *9*, 2611-2619.

Comings, D.E. (1980). Arrangement of chromatin in the nucleus. Hum. Genet. *53*, 131-143.

Cremer, T., *et al.* (1993). Role of chromosome territories in the functional compartmentalization of the cell nucleus. Cold Spring Harbor Symp. Quant. Biol. *58*, 777-792.

Dernburg, A.F., Sedat, J.W., Cande, W.Z., and Bass, H.W. (1995). Cytology of telomeres. In: Telomeres, ed. E.H. Blackburn and C.W. Greider, Cold Spring Harbor, NY: Cold Spring Harbor Laboratory Press, 295-338.

DuPraw, E.J. (1965). The organization of nuclei and chromosomes in honeybee embryonic cells. Proc. Natl. Acad. Sci. USA *53*, 161-168.

Ellison, J.R., and Howard, G.C. (1981). Non-random position of the A-T rich DNA sequences in early embryos of *Drosophila virilis*. Chromosoma *83*, 555-561.

Ferguson, M., and Ward, D.C. (1992). Cell cycle-dependent chromosomal movement in pre-mitotic human T-lymphocyte nuclei. Chromosoma *101*, 96-106.

Foe, V.E., and Alberts, B.M. (1985). Reversible chromosome condensation induced in *Drosophila* embryos by anoxia: visualization of interphase nuclear organization. J. Cell Biol. *100*, 1623-1636.

Foe, V.E., Odell, G.M., and Edgar, B.A. (1993). Mitosis and morphogenesis in the *Drosophila* embryo: point and counterpoint. In: The Development of *Drosophila melanogaster*, ed. M. Bate and A. Martinez Arias, Cold Spring Harbor, NY: Cold Spring Harbor Laboratory Press, 149-300.

Foisner, R., and Gerace, L. (1993). Integral membrane proteins of the nuclear envelope interact with lamins and chromosomes, and binding is modulated by mitotic phosphorylation. Cell *73*, 1267-1279.

Gasser, S.M., and Laemmli, U.K. (1986). Cohabitation of scaffold binding regions with upstream/enhancer elements of three developmentally regulated genes of *D. melanogaster*. Cell *46*, 521-530.

Glass, C.A., Glass, J.R., Taniura, H., Hasel, K.W., Blevitt, J.M., and Gerace, L. (1993). The α-helical rod domain of human lamins A and C contains a chromatin binding site. EMBO J. *12*, 4413-4424.

Glass, J.R., and Gerace, L. (1990). Lamins A and C bind and assemble at the surface of mitotic chromosomes. J. Cell Biol. *111*, 1047-1057.

Hartl, D.L., Nurminsky, D.I., Jones, R.W., and Lozovskaya, E.R. (1994). Genome structure and evolution in *Drosophila*: applications of the framework P1 map. Proc. Natl. Acad. Sci. USA *91*, 6824-6829.

Hassan, A.B., Errington, R.J., White, N.S., Jackson, D.A., and Cook, P.R. (1994). Replication and transcription sites are colocalized in human cells. J. Cell Sci. *107*, 425-434.

Hilliker, A.J., and Appels, R. (1989). The arrangement of interphase chromosomes: structural and functional aspects. Exp. Cell Res. *185*, 267-318.

Hiraoka, Y., Agard, D.A., and Sedat, J.W. (1990a). Temporal and spatial coordination of chromosome movement, spindle formation, and nuclear envelope breakdown during prometaphase in *Drosophila melanogaster* embryos. J. Cell Biol. *111*, 2815-2828.

Hiraoka, Y., Dernburg, A.F., Parmelee, S.J., Rykowski, M.C., Agard, D.A., and Sedat, J.W. (1993). The onset of homologous chromosome pairing during *Drosophila melanogaster* embryogenesis. J. Cell Biol. *120*, 591-600.

Hiraoka, Y., Minden, J.S., Swedlow, J.R., Sedat, J.W., and Agard, D.A. (1989). Focal points for chromosome condensation and decondensation revealed by three-dimensional in vivo time-lapse microscopy. Nature *342*, 293-296.

Hiraoka, Y., Rykowski, M.C., Lefstin, J.A., Agard, D.A., and Sedat, J.W. (1990b). Three-dimensional organization of chromosomes studied by in situ hybridization and optical sectioning microscopy. Proc. Society of Photooptical Instrumentation Engineers *1205*, 11-19.

Hiraoka, Y., Swedlow, J.R., Paddy, M.R., Agard, D.A., and Sedat, J.W. (1991). Three-dimensional multiple-wavelength fluorescence microscopy for the structural analysis of biological phenomena. Semin. Cell Biol. *2*, 153-165.

Hochstrasser, M., Mathog, D., Gruenbaum, Y., Saumweber, H., and Sedat, J.W. (1986). Spatial organization of chromosomes in the salivary gland nuclei of *Drosophila melanogaster*. J. Cell Biol. *102*, 112-123.

Hochstrasser, M., and Sedat, J.W. (1987). Three-dimensional organization of *Drosophila melanogaster* interphase nuclei. II. Chromosome spatial organization and gene regulation. J. Cell Biol. *104*, 1471-1483.

Hoefers, C., Baumann, P., Hummer, G., Jovin, T.M., and Arndt-Jovin, D.J. (1993). The localization of chromosome domains in human interphase nuclei: three-dimensional distance determinations of fluorescence in situ hybridization signals from confocal laser scanning microscopy. Bioimaging *1*, 96-106.

Hutchison, N., and Weintraub, H. (1985). Localization of DNAase I-sensitive sequences to specific regions of interphase nuclei. Cell *43*, 471-482.

Izaurralde, J., Mirkovitch, J., and Laemmli, U.K. (1988). Interaction of DNA with nuclear scaffolds in vitro. J. Mol. Biol. *200*, 111-125.

Jackson, D.A., Dickinson, P., and Cook, P.R. (1990). Attachment of DNA to the nucleoskeleton of HeLa cells examined using physiological conditions. Nucleic Acids Res. *18*, 4385-4393.

James, T.C., Eissenberg, J.C., Craig, C., Dietrich, V., Hobson, A., and Elgin, S.C.R. (1989). Distribution patterns of HP1, a heterochromatin-associated nonhistone chromosomal protein of *Drosophila*. Eur. J. Cell Biol. *50*, 170-180.

Kellum, R., and Schedl, P. (1992). A group of scs elements function as domain boundaries in an enhancer-blocking assay. Mol. Cell. Biol. *12*, 2424-2431.

Lawrence, J.B., Villnave, C.A., and Singer, R.H. (1988). Sensitive high-resolution chromatin and chromosome mapping in situ: presence and orientations of two closely integrated copies of EBV in a lymphoma line. Cell *52*, 51-61.

Lebkowski, J.S., and Laemmli, U.K. (1982). Non-histone proteins and long-range organization of HeLa interphase DNA. J. Mol. Biol. *156*, 325-344.

Lohe, A.R., Hilliker, A.J., and Roberts, P.A. (1993). Mapping simple repeated DNA sequences in heterochromatin of *Drosophila melanogaster*. Genetics *134*, 1149-1174.

Loidl, J. (1990). The initiation of meiotic chromosome pairing: the cytological view. Genome *33*, 759-770.

Luderus, M.E., den Blaauwen, J.L., de Smit, O.J., Compton, D.A., and van Driel, R. (1994). Binding of matrix attachment regions to lamin polymers involves single-stranded regions and the minor groove. Mol. Cell. Biol. *14*, 6297-6305.

Luderus, M.E., de Graaf, A., Mattia, E., den Blaauwen, J.L, Grande, M.A., de Jong, L., and van Driel, R. (1992). Binding of matrix attachment regions to lamin B. Cell *70*, 949-959.

Manuelidis, L., and Borden, J. (1988). Reproducible compartmentalization of individual chromosome domains in human CNS cells revealed by in situ hybridization and three-dimensional reconstruction. Chromosoma *96*, 396-410.

Mathog, D., Hochstrasser, M., Gruenbaum, Y., Saumweber, H., and Sedat, J. (1984). Characteristic folding pattern of polytene chromosomes in *Drosophila* salivary gland nuclei. Nature *308*, 414-421.

Murray, A.B., and Davies, H.G. (1979). Three-dimensional reconstruction of the chromatin bodies in the nuclei of mature erythrocytes from the newt *Triturus cristatus*: the number of nuclear envelope-attachment sites. J. Cell Sci. *35*, 59-66.

Paddy, M.R., Belmont, A.S., Saumweber, H., Agard, D.A., and Sedat, J.W. (1990). Interphase nuclear envelope lamins form a discontinuous network that interacts with only a fraction of the chromatin in the nuclear periphery. Cell *62*, 89-106.

Palladino, F., Laroche, T., Gilson, E., Axelrod, A., Pillus, L., and Gasser, S.M. (1993). SIR3 and SIR4 proteins are required for the positioning and integrity of yeast telomeres. Cell *75*, 543-555.

Papoulis, A. (1990). Probability & Statistics, Eagle Cliffs, NJ: Prentice-Hall, 332.

Pimpinelli, S., and Dimitri, P. (1989). Cytogenetic analysis of segregation distortion in *Drosophila melanogaster*: the cytological organization of the Responder (Rsp) locus. Genetics *121*, 765-772.

Press, W.H., Flannery, B.P., Teukolsky, S.A., and Vetterling, W.T. (1989). Numerical Recipes in Pascal. Cambridge, United Kingdom: Cambridge University Press, 224-226.

Purcell, C., Mashiko, T., Odaka, K., and Ueno, K. (1991). Describing head shape with surface harmonic expansions. IEEE Trans. Biomed. Eng. *38*, 303-305.

Quick, P. (1980). Junctions of polytene chromosomes and the inner nuclear membrane. Experientia *36*, 456-457.

Rastelli, L., Chan, C.G., and Pirrotta, V. (1993). Related chromosome binding sites for zeste, suppressors of zeste, and Polycomb group proteins in *Drosophila* and their dependence on Enhancer of zeste function. EMBO J. *12*, 1513-1522.

Sambrook, J., Fritsch, E.F., and Maniatis, T. (1989). Molecular Cloning: A Laboratory Manual, Cold Spring Harbor, NY: Cold Spring Harbor Laboratory Press.

Spector, D.L. (1993). Macromolecular domains within the cell nucleus. Annu. Rev. Cell Biol. *9*, 265-315.

Sukegawa, J., and Blobel, G. (1993). A nuclear pore complex protein that contains zinc finger motifs, binds DNA, and faces the nucleoplasm. Cell *72*, 29-38.

Telenius, H., Carter, N.P., Bebb, C.E., Nordenskjold, M., Ponder, B.A., and Tunnacliffe, A. (1992). Degenerate oligonucleotide-primed PCR: general amplification of target DNA by a single degenerate primer. Genomics *13*, 718-725.

Udvardy, A., Maine, E., and Schedl, P. (1985). The 87A7 chromomere: identification of novel chromatin structures flanking the heat shock locus that may define the boundaries of higher order domains. J. Mol. Biol. *185*, 341-355.

van Dekken, H., Pinkel, D., Mulliken, J., Trask, B., van den Engh, G., and Gray, J. (1989). Three-dimensional analysis of the organization of human chromosome domains in human and human-hamster hybrid interphase nuclei. J. Cell Sci. *94*, 299-306.

van Dekken, H., van Rotterdam, A., Jonker, R., van der Voort, H.T.M., Brakenhoff, G.J., and Bauman, J.G.J. (1990). Confocal microscopy as a tool for the study of the intranuclear topography of chromosomes. J. Microscopy *158*, 207-214.

Vourc'h, C., Taruscio, D., Boyle, A.L., and Ward, D.C. (1993). Cell cycle-dependent distribution of telomeres, centromeres, and chromosome-specific subsatellite domains in the interphase nucleus of mouse lymphocytes. Exp. Cell Res. *205*, 142-151.

Wakimoto, B.T., and Hearn, M.G. (1990). The effects of chromosome rearrangements on the expression of the heterochromatic genes in chromosome 2L of *Drosophila melanogaster*. Genetics *125*, 141-154.

Wiese, C., and Wilson, K. (1993). Nuclear membrane dynamics. Curr. Opin. Cell Biol. *5*, 387-394.

Worman, H.J., Evans, C.P., and Blobel, G. (1990). The lamin B receptor of the nuclear envelope inner membrane: a polytopic protein with eight potential transmembrane domains. J. Cell Biol. *111*, 1535-1542.

Wu, C.I., Lyttle, T.W., Wu, M.L., and Lin, G.F. (1988). Association between a satellite DNA sequence and the responder of segregation distorter in *D. melanogaster*. Cell *54*, 179-189.

Yokota, H., van den Engh, G., Hearst, J.E., Sachs, R.K., and Trask, B.J. (1995). Evidence for the organization of chromatin in megabase pair-sized loops arranged along a random walk path in the human G0/G1 interphase nucleus. J. Cell Biol. *130*, 1239-1250.

Yuan, J., Simos, G., Blobel, G., and Georgatos, S.D. (1991). Binding of lamin A to polynucleosomes. J. Biol. Chem. *266*, 9211-9215.

Zalensky, A.O., Allen, M.J., Kobayashi, A., Zalenskaya, I.A., Balhron, R., and Bradbury, E.M. (1995). Well-defined genome architecture in the human sperm nucleus. Chromosoma *103*, 577-590.

Zhimulev, I.F., Semeshin, V.F., Kulichkov, V.A., and Belyaeva, E.S. (1982). Intercalary heterochromatin in *Drosophila*. I. Localization and general characteristics. Chromosoma *87*, 197-228.